# Airway smooth muscle prostaglandin-EP1 receptors directly modulate β2–adrenergic receptors within a unique heterodimeric complex

Dennis W. McGraw, … , Khalid F. Almoosa, Stephen B. Liggett

**Research Article**   **Inflammation**

Multiple and paradoxical effects of airway smooth muscle (ASM) 7-transmembrane–spanning receptors activated during asthma, or by treatment with bronchodilators such as $\beta_2$–adrenergic receptor ($\beta_2$AR) agonists, indicate extensive receptor crosstalk. We examined the signaling of the prostanoid-EP$_1$ receptor, since its endogenous agonist prostaglandin E$_2$ is abundant in the airway, but its functional implications are poorly defined. Activation of EP$_1$ failed to elicit ASM contraction in mouse trachea via this $G_{\alpha q}$-coupled receptor. However, EP$_1$ activation markedly reduced the bronchodilatory function of $\beta_2$AR agonist, but not forskolin, indicating an early pathway interaction. Activation of EP$_1$ reduced $\beta_2$AR-stimulated cAMP in ASM but did not promote or augment $\beta_2$AR phosphorylation or alter $\beta_2$AR trafficking. Bioluminescence resonant energy transfer showed EP$_1$ and $\beta_2$AR formed heterodimers, which were further modified by EP$_1$ agonist. In cell membrane [$^{35}$S]GTP$\gamma$S binding studies, the presence of the EP$_1$ component of the dimer uncoupled $\beta_2$AR from $G_{\alpha s}$, an effect accentuated by EP$_1$ agonist activation. Thus alone, EP$_1$ does not appear to have a significant direct effect on airway tone but acts as a modulator of the $\beta_2$AR, altering $G_{\alpha s}$ coupling via steric interactions imposed by the EP$_1$:$\beta_2$AR heterodimeric signaling complex and ultimately affecting $\beta_2$AR-mediated bronchial relaxation. This mechanism may contribute to β-agonist resistance found in asthma.

**Find the latest version:**

# Airway smooth muscle prostaglandin-EP$_1$ receptors directly modulate β$_2$–adrenergic receptors within a unique heterodimeric complex

Dennis W. McGraw,[1] Kathryn A. Mihlbachler,[2] Mary Rose Schwarb,[2] Fahema F. Rahman,[1] Kersten M. Small,[1] Khalid F. Almoosa,[1] and Stephen B. Liggett[2]

[1]Pulmonary Division, Department of Medicine, University of Cincinnati College of Medicine, Cincinnati, Ohio, USA. [2]Cardiopulmonary Genomics Program, University of Maryland School of Medicine, Baltimore, Maryland, USA.

**Multiple and paradoxical effects of airway smooth muscle (ASM) 7-transmembrane–spanning receptors activated during asthma, or by treatment with bronchodilators such as β$_2$–adrenergic receptor (β$_2$AR) agonists, indicate extensive receptor crosstalk. We examined the signaling of the prostanoid-EP$_1$ receptor, since its endogenous agonist prostaglandin E$_2$ is abundant in the airway, but its functional implications are poorly defined. Activation of EP$_1$ failed to elicit ASM contraction in mouse trachea via this G$_{\alpha q}$-coupled receptor. However, EP$_1$ activation markedly reduced the bronchodilatory function of β$_2$AR agonist, but not forskolin, indicating an early pathway interaction. Activation of EP$_1$ reduced β$_2$AR-stimulated cAMP in ASM but did not promote or augment β$_2$AR phosphorylation or alter β$_2$AR trafficking. Bioluminescence resonant energy transfer showed EP$_1$ and β$_2$AR formed heterodimers, which were further modified by EP$_1$ agonist. In cell membrane [$^{35}$S]GTPγS binding studies, the presence of the EP$_1$ component of the dimer uncoupled β$_2$AR from G$_{\alpha s}$, an effect accentuated by EP$_1$ agonist activation. Thus alone, EP$_1$ does not appear to have a significant direct effect on airway tone but acts as a modulator of the β$_2$AR, altering G$_{\alpha s}$ coupling via steric interactions imposed by the EP$_1$:β$_2$AR heterodimeric signaling complex and ultimately affecting β$_2$AR-mediated bronchial relaxation. This mechanism may contribute to β-agonist resistance found in asthma.**

## Introduction

The 7-transmembrane–spanning (7-TM–spanning) receptors represent the largest signaling family in the genome. We estimate that the lung expresses 25–50 7-TM receptors in airway epithelial cells, airway smooth muscle (ASM), pulmonary vasculature, alveolar walls, and resident immune cells (1). In regard to asthma, several 7-TM receptors play established roles in bronchoconstriction (e.g., M$_3$-muscarinic receptor) and bronchodilation (e.g., β$_2$–adrenergic receptor [β$_2$AR]). Despite identification of the endogenous ligands and receptor localization, there are a number of 7-TM receptors expressed in the airway whose functions are unknown, or appear to function paradoxically, based on recombinantly expressed receptors in model cell systems. This lack of understanding of receptor function has impeded our ability to ascertain the role of these ligands (some of which are markedly increased in asthma) in the relaxation/contraction of ASM; thus the mechanistic basis of bronchial hyperreactivity and bronchoconstriction in asthma remains only partially understood. In many cases the basis for incomplete mechanistic information can be attributed to the nature of recombinant expression systems, which may not take into account multiple receptor subtypes, receptor/receptor interactions, crosstalk via second messengers, or subcellular localization of receptors and specific effectors.

These issues are particularly obvious when one considers the biologic actions of prostaglandin E$_2$ (PGE$_2$), which, via at least 4 receptor subtypes (EP$_1$–EP$_4$), can evoke multiple signals. By activation of the G$_s$-coupled EP$_2$ receptor, PGE$_2$ can evoke ASM relaxation (2). However, blockade of PGE$_2$ production leads to partial reversal of β$_2$AR desensitization in the context of inflammation (3), and thus PGE$_2$ may promote bronchoconstriction via desensitization of β$_2$AR function or by activation of the G$_q$-coupled EP$_1$ receptor. PGE$_2$ is produced by ASM, airway epithelial cells, and inflammatory cells and is the most abundant prostanoid in epithelial lining fluid (4–6). However, EP$_1$-mediated signal transduction and its effect on airway responsiveness remains unclear. We show here a unique function of the EP$_1$ receptor in ASM, which to our knowledge has not been previously described for 7-TM receptors. The EP$_1$ receptor itself, despite its coupling to inositol 1,4,5-tri-phosphate (IP$_3$) and intracellular calcium ([Ca$^{2+}$]$_i$), failed to exert the expected bronchoconstrictive response. Instead, EP$_1$ receptor activation modulated β$_2$AR function via formation of a heterodimeric complex that directly decreased β$_2$AR coupling to G$_{\alpha s}$ in an EP$_1$ receptor, agonist-dependent, fashion.
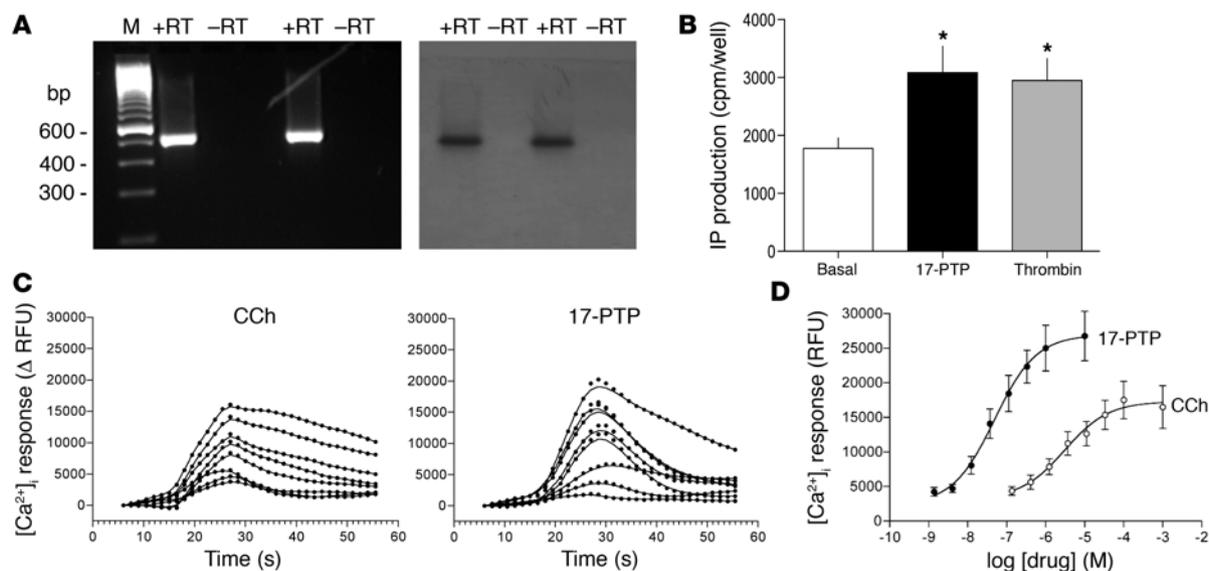
## Results

*EP$_1$ receptor activation in isolated and intact ASM.* The biologic actions of PGE$_2$ are potentially mediated by multiple receptor subtypes that differentially couple to G$_q$, G$_i$, and G$_s$. Although a relaxant

---

**Figure 1**
$EP_1$ receptor expression and signal transduction in murine ASM cells. (**A**) $EP_1$ gene expression was detected in cultured murine ASM cells by RT-PCR. The 501-bp product (left) corresponding to sequence from the $EP_1$ receptor open reading frame was only detected in reactions that included reverse transcriptase (+RT) and hybridized by Southern blots to an $EP_1$-specific probe (right). (**B**) The $EP_1$-selective agonist 17-PTP (1 μM) stimulated inositol phosphate (IP) production in murine ASM ~70% above basal levels ($n = 4$). Thrombin-stimulated inositol phosphate production was used for a positive control. *$P < 0.05$ versus basal. (**C**) Both 17-PTP and acetylcholine-stimulated $[Ca^{2+}]_i$ transients in ASM cells. Shown is a representative experiment using the doses shown in **D**. (**D**) Maximal agonist-stimulated $[Ca^{2+}]_i$ transients in ASM cells exposed to the indicated doses of agonists. Data are mean ± SEM of 5 experiments. Cch, carbachol; RFU, relative fluorescence units.

action of $PGE_2$, mediated via the $EP_2$ isoform in ASM, has been documented (7), the extent to which $PGE_2$ couples to the other subtypes in ASM, particularly the potentially probronchoconstrictive $G_q$-coupled $EP_1$ receptor, is not established. $EP_1$-specific RT-PCR was carried out on murine ASM cells in culture (Figure 1A). A single product of the expected molecular size was obtained, and Southern blots with an $EP_1$-specific oligonucleotide hybridized to the product. Sequencing further confirmed the product as the murine $EP_1$ receptor (GenBank accession no. NM_013641). With regard to signal transduction, the $EP_1$-specific agonist 17-phenyl trinor-$PGE_2$ (17-PTP) was found to stimulate inositol phosphate production (Figure 1B) and $[Ca^{2+}]_i$ transients (Figure 1C). Of note, maximal activation of the $EP_1$ receptor by 17-PTP stimulated $[Ca^{2+}]_i$ to a greater extent, and with greater potency, than the $M_3$-muscarinic agonist carbachol (Figure 1D). These findings confirmed $EP_1$ receptor expression in ASM cells and that its activation by agonists resulted in $IP_3$ and $[Ca^{2+}]_i$ turnover as assessed in whole cells. Because these effectors mediate 7-TM receptor contraction of ASM, the data suggested that the $EP_1$ receptor would likely promote airway contraction.

Excised mouse tracheal ring preparations were utilized to ascertain the effects of $EP_1$ activation on active force generation in the intact airway. However, despite its ability to stimulate $IP_3$ and $[Ca^{2+}]_i$ turnover in ASM, 17-PTP caused no detectable contraction of tracheal rings even at concentrations up to 10 μM (Figure 2A). Since 17-PTP did not directly effect ASM tone, we next investigated whether $EP_1$ receptor activation could modify the response to another contractile agonist acting through $G_{\alpha q}$. For these studies, tracheal rings were pretreated with 1 μM 17-PTP for 15 minutes prior to contraction with various concentrations of acetylcholine (Figure 2A). The maximal acetylcholine response in the absence

(26 ± 5.3 mN) or presence (26 ± 4.8 mN) of $EP_1$ coactivation was not different, nor was the $EC_{50}$ for the response (91 ± 11 versus 82 ± 15 μM, respectively). We next considered whether $EP_1$ receptor activation alters ASM relaxation. The efficacy and potency of the βAR agonist isoproterenol to relax acetylcholine-constricted ASM in the presence and absence of $EP_1$ receptor activation was ascertained. Tracheal rings were first treated with vehicle or 1 μM 17-PTP for 15 minutes, contracted continuously with 10 μM acetylcholine, and exposed to increasing concentrations of isoproterenol. In the presence of vehicle, isoproterenol caused a dose-dependent relaxation with an $EC_{50}$ of 23.4 ± 4.8 nM and a maximal reduction in force of 36.6% ± 2.9% (Figure 2B). However, following pretreatment with 17-PTP, a marked reduction in βAR-mediated relaxation was observed, with isoproterenol evoking only 17.1% ± 2.4% relaxation ($n = 6$; $P < 0.001$; Figure 2B). Of note, the $EC_{50}$ for isoproterenol was also increased under these conditions to 58.2 ± 6.1 nM ($P < 0.001$). As shown in Figure 2C, this same βAR desensitization effect of 17-PTP was observed when tracheal rings were contracted by 60 mM KCl. The endogenous $EP_1$ receptor agonist is $PGE_2$, which activates other EP receptors and thus under physiologic conditions could evoke an effect that dominates airway responses over the $EP_1$-specific phenotype we observed. We therefore studied the effect of pretreatment with 10 nM $PGE_2$ (which evokes only ~15% relaxation) using the same protocol as for 17-PTP. As shown in Figure 2D, $PGE_2$ also evoked a loss of isoproterenol-mediated relaxation, amounting to an approximate 25% desensitization. This lower amount of desensitization (compared with 17-PTP pretreatment) may be due to the combined relaxant effect of $PGE_2$ and isoproterenol.

Given that mouse trachea has a mixed population of $β_1AR$ and $β_2AR$ subtypes (8), the 17-PTP effect was also assessed using the
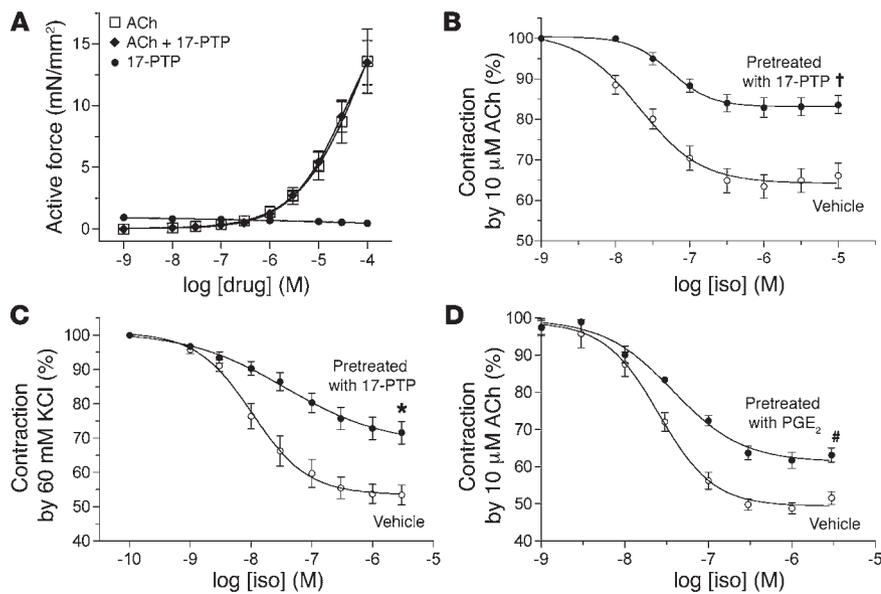
**Figure 2**
Effect of EP$_1$ receptor activation on ASM contraction and relaxation. (**A**) Concentrations of 17-PTP up to 10 μM caused no significant contraction of murine tracheal rings and did not enhance acetylcholine-mediated (Ach) contraction. Data are mean ± SEM of 4 experiments. (**B**) Pretreatment of tracheal rings with 1 μM 17-PTP for 15 minutes reduced both the potency (EC$_{50}$ increased) and efficacy of isoproterenol-mediated (Iso) relaxation of tracheal rings contracted with 10 μM acetylcholine. Data are mean ± SEM of 6 experiments. †$P = 0.001$ versus vehicle-treated rings. (**C**) The inhibitory effect of 17-PTP on isoproterenol-mediated relaxation was also present when the tracheal rings were contracted with 60 mM KCl. Data are mean ± SEM of 8 experiments. *$P < 0.05$ versus vehicle-treated rings. (**D**) Pretreatment of tracheal rings with 10 nM PGE$_2$ evokes desensitization of isoproterenol-mediated relaxation. Data are mean ± SEM of 5 experiments. #$P < 0.02$ versus vehicle-treated rings.
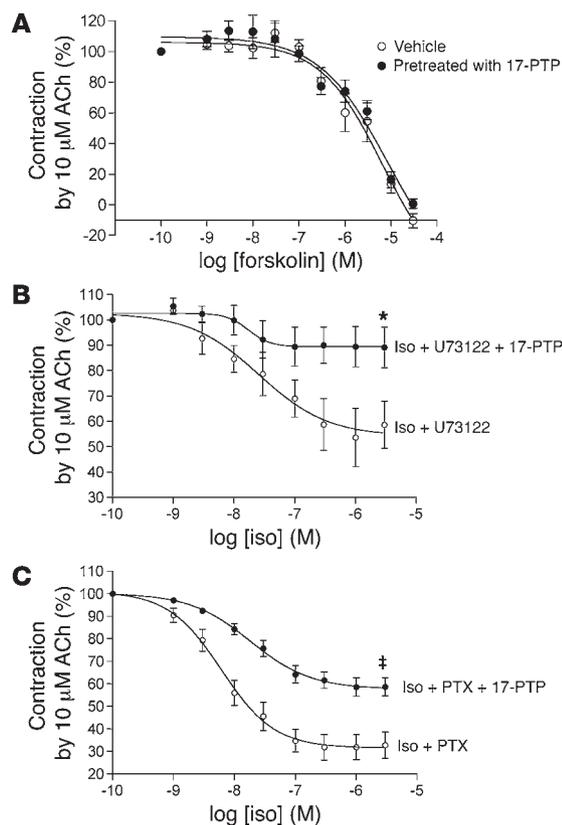
relatively β$_2$AR subtype-specific agonist formoterol. Under these conditions, 17-PTP evoked a 55% ± 5% desensitization of formoterol-mediated relaxation, indicating a 17-PTP effect on β$_2$AR (the predominant βAR subtype of human tracheal ASM). To determine whether the inhibitory effect of 17-PTP extended to other ASM relaxants, we performed analogous experiments with forskolin, which directly activates adenylyl cyclase, mimicking a G$_s$-coupled receptor. However, unlike the response with isoproterenol, pretreatment with 17-PTP had no effect on the maximal response or the EC$_{50}$ (Figure 3A). Given that the EP$_1$ receptor couples to G$_{\alpha q}$, we considered that second messengers generated from phospholipase C (PLC) activation may be involved in the apparent crosstalk between β$_2$AR and EP$_1$ receptors. However, pretreatment with the PLC inhibitors U73122 (5 μM; Figure 3B) and Et-18-OCH$_3$ (10 μM; data not shown) failed to alter the 17-PTP effect. β$_2$ARs have also been shown in some cells to couple to G$_{\alpha i}$ (9), which may act to oppose G$_{\alpha s}$-mediated signaling. Treatment of tracheal rings with pertussis toxin, however, had no effect on the EP$_1$-mediated β$_2$AR desensitization (Figure 3C), indicating that enhanced G$_i$ coupling was an unlikely mechanism. Finally, the β$_2$AR desensitization phenotype evoked by EP$_1$ activation was not altered by pretreatment with 100 μM of the NO inhibitor L-NAME (51.2% ± 6.8% desensitization) or 10 μM of the cyclooxygenase inhibitor indomethacin (57% ± 5% desensitization).

*Desensitization of β$_2$AR by EP$_1$ receptor activation.* The inhibitory effect of 17-PTP on isoproterenol-mediated relaxation observed

in the tracheal ring studies indicated functional interplay between the EP$_1$ and β$_2$AR signal transduction pathways. Additionally, the absence of a significant EP$_1$ effect on forskolin-mediated relaxation and no change in phenotype observed with PLC inhibition suggested that this interaction could potentially occur at the level of the β$_2$AR itself. The effect of 17-PTP on isoproterenol-stimulated cAMP production was determined in isolated ASM cells. In the absence of 17-PTP, 1 μM isoproterenol stimulated cAMP to 88.0% ± 16.3% of the maximum level obtained with 10 μM forskolin. However, when cells were pretreated with 1 μM 17-PTP for 15 minutes prior to isoproterenol stimulation, cAMP production was reduced to 37.0% ± 3.9% ($n = 4$; $P = 0.02$) of the forskolin response (Figure 4A). Taken together with the tracheal ring data, these results indicated an interplay between the EP$_1$ receptor and β$_2$AR, with activation of the former resulting in decreased function of the latter. Two processes that we considered potential mechanisms to account for uncoupling of β$_2$AR signal transduction within the time frame of minutes included (a) enhanced loss of cell surface receptors due to internalization and (b) enhanced isoproterenol-stimulated β$_2$AR phosphorylation due to EP$_1$ activation or phosphorylation of the β$_2$AR by EP$_1$ activation via PKC. To ascertain whether EP$_1$ activation altered the extent or rate of agonist-mediated β$_2$AR internalization, we performed radioligand binding on intact ASM cells with the hydrophilic radioligand [$^3$H]-CGP-12177. Since this ligand does not enter intact cells (10), a decrease in binding occurs when surface receptors are internalized. Thus, as expected for agonist-promoted internalization of the β$_2$AR, exposure of ASM cells to 1 μM isoproterenol caused a time-dependent decrease in [$^3$H]-CGP-12177 binding sites of 39.1% ± 5.7% after 30 minutes (Figure 4B). Pretreatment of cells with 1 μM 17-PTP for 15 minutes had no effect on isoproterenol-stimulated internalization (37.4% ± 3.6%; $n = 5$). We next examined the potential for 17-PTP to promote phosphorylation of the β$_2$AR. For the phosphorylation experiments, human embryonic kidney (HEK) cells transiently cotransfected with plasmids so as to express the EP$_1$ receptor and FLAG-tagged β$_2$AR were loaded with $^{32}$P-orthophosphate. Cells were treated with vehicle, isoproterenol, 17-PTP, phorbol-12-myristate-13-acetate (a positive control for PKC-mediated event), or isoproterenol plus 17-PTP. β$_2$AR was purified by FLAG immunoprecipitation. As shown in Figure 4C, isoproterenol evoked robust phosphorylation of the β$_2$AR, while no detectable phosphorylation over background was noted with 17-PTP exposure alone. Importantly, the extent of isoproterenol–promoted β$_2$AR phosphorylation was not altered by 17-PTP (48 ± 4.5 relative units versus 42 ± 4.2 relative units in the presence and absence of 17-PTP, respectively; $n = 5$; $P = $ NS).

*β$_2$ARs and EP$_1$ receptors form heterodimers.* Since these well-defined short-term mechanisms of receptor regulation and crosstalk were not at play during EP$_1$-induced desensitization of β$_2$AR, we con-

**Figure 3**
Characterization of EP$_1$ receptor–promoted desensitization of β$_2$AR-mediated ASM relaxation. (**A**) No effect of 17-PTP pretreatment was observed on forskolin-mediated ASM relaxation, indicating that the site of EP$_1$ modulation is likely proximal to adenylyl cyclase ($n = 4$). (**B**) Inhibition of phospholipase C (PLC) with U73122 failed to alter the 17-PTP–evoked desensitization of isoproterenol-mediated ASM relaxation. *$P < 0.05$ versus vehicle-treated rings ($n = 4$). (**C**) Ablation of receptor-G$_{\alpha i}$ coupling with pertussis toxin (PTX) had no effect on the 17-PTP–evoked desensitization of isoproterenol-mediated ASM relaxation. ‡$P < 0.01$ versus rings not treated with 17-PTP ($n = 4$).

tein (YFP). As described in detail elsewhere (11–13), this approach takes advantage of a signal produced by the energy donor moiety (Rluc) acting on the energy acceptor (YFP) when the two are in very close proximity. As shown in Figure 5B, studies carried out in HEK 293 cells transfected to express β$_2$AR-Rluc and EP$_1$-YFP (see Methods) indeed revealed a BRET signal, as indicated by the perturbation of the emission spectrum at 530 nM. To verify that this represented oligomer formation, rather than a "pseudo-BRET" signal (11) due to random collisions of overexpressed receptors, studies were carried out with multiple levels of expression (altering the β$_2$AR-Rluc/EP$_1$-YFP ratio). As expected under conditions of dimer formation, the BRET signal saturated, with a calculated maximal ratio (BRET$_{max}$) of 0.49 ± 0.04 and a BRET$_{50}$ of 2.97 ± 0.56 (Figure 5C). In contrast, in experiments utilizing cotransfections of β$_2$AR-Rluc and a YFP fusion with the γ-aminobutyric acid receptor subtype bR2 (GABAb R2–YFP) a small signal was observed, as was the case with cotransfections of C-C chemokine receptor 5–Rluc (CCR5-Rluc) and β$_2$AR-YFP (Figure 5D). These low-level signals and a lack of saturation (data not shown) were consistent with prior observations that neither the GABAb R2 nor CCR5 recep-

sidered an alternative hypothesis, which was that the 2 receptors formed heterodimers. We also considered whether agonist activation of the EP$_1$ receptor directly affected the receptor/receptor interaction within the complex, altering β$_2$AR coupling to G$_{\alpha s}$. As a screen for such a complex in ASM cells, fluorescence microscopy was carried out using β$_2$AR- and EP$_1$-specific primary antibodies. Secondary antibodies provided for red (β$_2$AR) and green (EP$_1$) signals. Merged images revealed yellow signals consistent with areas of colocalization of these 2 receptors (Figure 5A). To rigorously assess the potential for heterodimer formation, bioluminescence resonant energy transfer (BRET) and coimmunoprecipitation studies were undertaken in transfected HEK 293 cells. BRET was carried out in living cells expressing 2 receptors having carboxyterminally fused Renilla luciferase (Rluc) or yellow fluorescent pro-
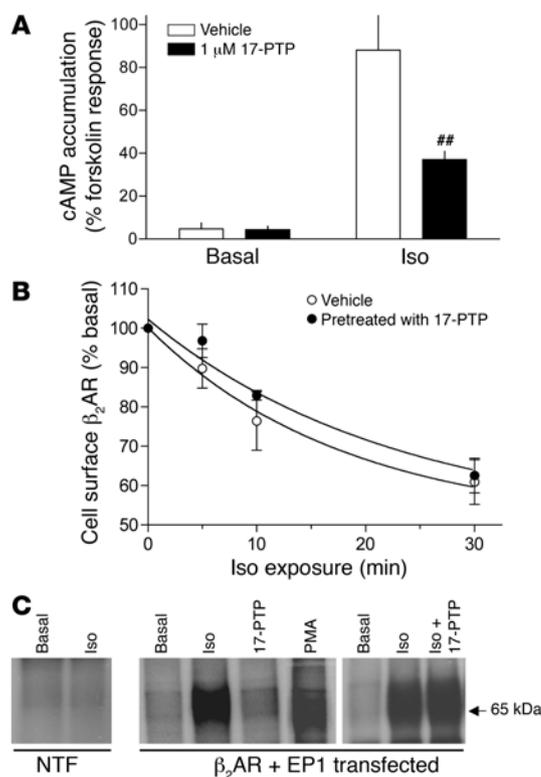


**Figure 4**
Effect of EP$_1$ receptor activation on β$_2$AR agonist–stimulated cAMP production, receptor sequestration and receptor phosphorylation. (**A**) Pretreatment of ASM cells with 17-PTP (1 μM) for 15 minutes reduced isoproterenol-stimulated cAMP production. Data are mean ± SEM of 4 experiments. ##$P = 0.02$ versus vehicle-treated cells. (**B**) Isoproterenol caused a time-dependent internalization of β$_2$AR in murine ASM cells over 30 minutes as assessed by whole-cell binding using the hydrophilic antagonist [³H]-CGP-12177; pretreatment with 17-PTP (1 μM for 15 min) had no effect on internalization. Data are mean ± SEM of 4 experiments. (**C**) EP$_1$ receptor activation failed to phosphorylate β$_2$AR or to alter isoproterenol-mediated β$_2$AR phosphorylation in HEK 293 cells transfected to express β$_2$AR and EP$_1$ receptors. Shown is a representative autoradiogram of 4 experiments. PMA, phorbol-12-myristate-13-acetate. NTF, nontransfected.
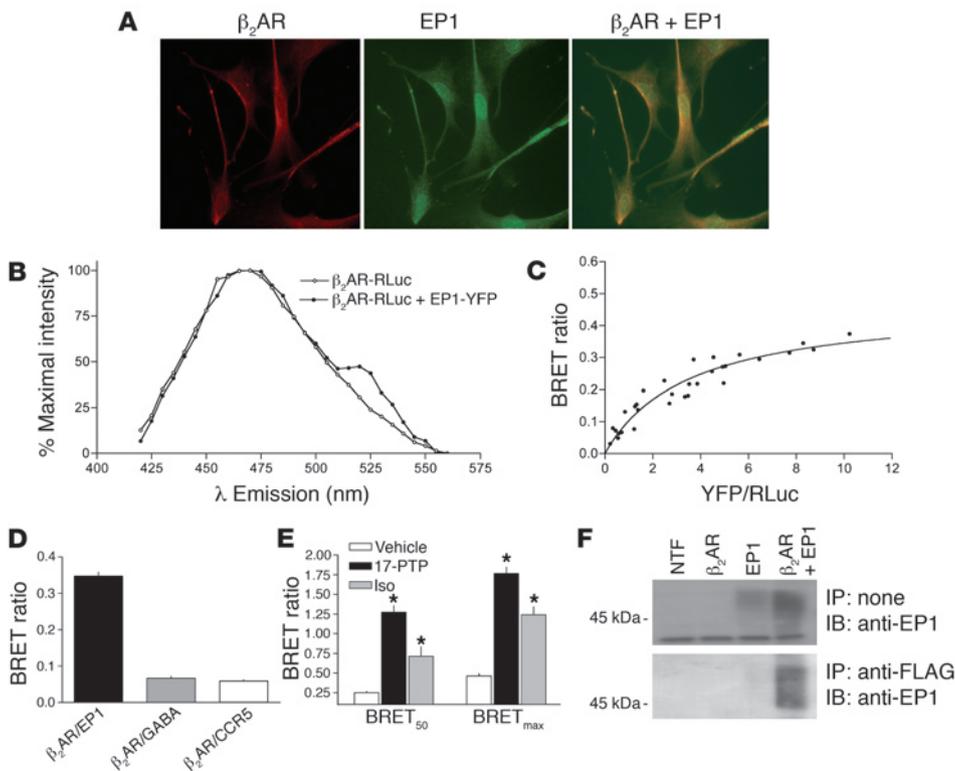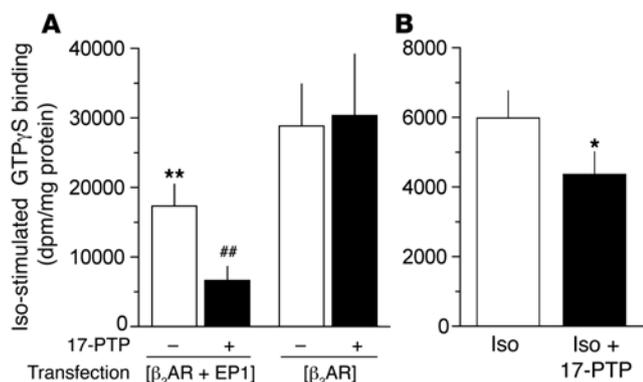
**Figure 5**
The EP$_1$ receptor and β$_2$AR form a heterodimer as assessed by BRET and coimmunoprecipitation. (**A**) Immunofluorescence microscopy revealed potential colocalization of EP$_1$ and β$_2$AR in ASM cells. Magnification, ×200. (**B**) The emission spectra of HEK 293 cells transfected with the β$_2$AR-Rluc fusion alone showed a single peak with a maximum at ~475 nm following addition of coelenterazine h (open symbols). However, a second peak was observed at ~530 nm when cells were cotransfected with the EP$_1$-YFP fusion construct (closed symbols). Shown is a representative experiment of 4. (**C**) The BRET ratios derived from HEK 293 cells transfected with a fixed amount of the donor β$_2$AR-Rluc reached saturation with increasing expression of the acceptor EP$_1$-YFP. Data shown are compiled from 12 experiments. (**D**) GABAb R2 and C-C chemokine receptor 5 (CCR5) failed to form heterodimers with β$_2$AR as indicated by low pseudo-BRET signals. (**E**) The BRET ratios of HEK 293 cells cotransfected with the β$_2$AR-Rluc and EP$_1$-YFP were increased by treatment with either the EP$_1$ agonist 17-PTP or the βAR agonist isoproterenol. *$P < 0.05$ versus untreated; $n = 4$. (**F**) Coimmunoprecipitation of FLAG-EP$_1$:β$_2$AR receptor complexes. HEK 293 cells were transfected with FLAG-β$_2$AR, EP$_1$ receptor, or both; membranes were solubilized; and proteins were immunoprecipitated with anti-FLAG antibody. Western blots of whole-cell lysates and immunoprecipitates were carried out with polyclonal EP$_1$ receptor antisera. Shown is a representative blot from 5 experiments.

tors form heterodimers with the β$_2$AR (13, 14). We next examined whether activation of the EP$_1$ receptor or the β$_2$AR altered the BRET signal. As shown in Figure 5E, treatment of cotransfected cells with 17-PTP or isoproterenol for 15 minutes prior to the addition of coelenterazine h increased the BRET signal in both cases. Given that most 7-TM dimers appear to be formed intracellularly and then expressed at the cell surface (11, 12, 15, 16), and given the short-term agonist exposure used in these experiments, we do not interpret these results as representing an increased number of dimers per se. Rather, the data are consistent with a conformational change that occurs (potentially in either receptor) when one receptor is bound by its agonist, which causes the Rluc and YFP moieties to move closer together. The magnitude of the agonist-promoted increase in BRET is not trivial, in that the BRET signal is proportional to the distance between the donor and acceptor by a factor of $10^6$ (11, 12, 15).

To further corroborate dimer formation, coimmunoprecipitation studies were carried out in HEK 293 cells transfected to express FLAG-β$_2$AR and the EP$_1$ receptor both alone and together. Immunoprecipitation was carried out with anti-FLAG antibody, and the precipitated proteins were fractionated on SDS-PAGE followed by Western blots using a polyclonal EP$_1$ antisera. As shown in Figure 5F, the EP$_1$ receptor migrated at approximately 45 kDa in Western blots of cell lysates using the EP$_1$ antisera. Upon immunoprecipitation with FLAG antibody, protein from cells transfected to express EP$_1$ or β$_2$AR showed no immunoreactivity with the EP$_1$ antisera. However, when the 2 receptors were cotransfected, a band of the appropriate molecular size was observed. Of note, the high–molecular weight bands, which could represent dimers, are often not resistant to SDS and are not typically visualized (14). These coimmunoprecipitation studies are thus consistent with the BRET results, indicating the presence of the EP$_1$:β$_2$AR heterodimer.

*EP$_1$:β$_2$AR heterodimer formation uncouples β$_2$AR from G$_{\alpha s}$.* Taken together, the above results indicated that the EP$_1$ receptor and the β$_2$AR exist as an oligomeric complex, with activation of the EP$_1$ receptor markedly desensitizing β$_2$AR signaling and physiologic function, and that such desensitization is not due to downstream second messenger feedback. This suggested that agonist activation of the EP$_1$ receptor within the dimer results in a steric effect on the β$_2$AR, altering its conformation in such a way as to directly affect β$_2$AR-G$_{\alpha s}$ interaction. To examine this, we studied agonist-promoted [$^{35}$S]GTPγS binding in cell membranes. This provided for direct quantitation of receptor–G protein interaction by measuring GTP turnover and, since it is performed with isolated membranes, was not affected by intracellular factors. In these studies, [$^{35}$S]GTPγS binding was carried out by incubating membranes from cells transfected to express G$_{\alpha s}$, β$_2$AR, and the EP$_1$ receptor with vehicle, isoproterenol alone, or isoproterenol with 17-PTP. In other studies, G$_{\alpha s}$ and β$_2$AR were expressed without the EP$_1$ receptor so as to ascertain β$_2$AR coupling to G$_{\alpha s}$ in the absence of the EP$_1$:β$_2$AR dimer. Expression levels of β$_2$AR in the β$_2$AR and EP$_1$ (3774 ± 815 fmol/mg) and β$_2$AR transfections (3367 ± 185 fmol/mg) were comparable. Net isoproterenol-stimulated [$^{35}$S]GTPγS binding is shown in Figure 6A. Incubation with 17-PTP resulted in a significant

**Figure 6**
EP$_1$ receptor activation uncouples the β$_2$AR from G$_s$. β$_2$AR coupling to G$_s$ was assessed by measuring isoproterenol-stimulated [$^{35}$S]GTPγS binding in membranes from COS-7 cells transfected with G$_{\alpha s}$ and the β$_2$AR, or with G$_{\alpha s}$ and β$_2$AR plus EP$_1$ (**A**) or mouse primary ASM cells (**B**). Reactions were performed with partially purified cell membranes. The [$^{35}$S]GTPγS bound to G$_{\alpha s}$ was recovered by immunoprecipitation with G$_{\alpha s}$ antibody as described in Methods. (**A**) The presence of 17-PTP in the reaction significantly reduced [$^{35}$S]GTPγS binding stimulated by isoproterenol in the transfected COS-7 cells, while the β$_2$AR expressed without the EP$_1$ had the greatest stimulation by isoproterenol. No effect of 17-PTP was observed on cells transfected to only express β$_2$AR. **P = 0.05 versus β$_2$AR only; ##P = 0.02 versus 17-PTP–untreated cells coexpressing β$_2$AR and EP$_1$ receptor. Shown are mean ± SEM from 6 experiments. (**B**) The presence of 17-PTP in the reaction decreased isoproterenol-stimulated [$^{35}$S]GTPγS binding in ASM cell membranes. *P < 0.05 versus isoproterenol in the absence of 17-PTP. Shown are mean ± SEM from 6 experiments. In both types of experiments, basal (non-agonist) binding was ~65% of isoproterenol-stimulated binding.

decrease in isoproterenol-stimulated binding, amounting to an approximately 60% reduction (n = 4; P = 0.02). Interestingly, the presence of the EP$_1$ receptor, even in the absence of its activation by agonist, decreased β$_2$AR coupling to G$_{\alpha s}$. As shown in Figure 6A, cells expressing β$_2$AR alone had the highest isoproterenol-stimulated [$^{35}$S]GTPγS binding, and as expected, 17-PTP had no effect in these cells. Additional studies were also carried out using ASM cell membranes (Figure 6B). Analogous to what was observed in the transfected cell studies, [$^{35}$S]GTPγS turnover was decreased when membranes were incubated with isoproterenol and 17-PTP compared with isoproterenol alone. These data then confirmed the concept of a direct interaction between the 2 receptors in the cell type of interest when the receptors were expressed at physiologic levels.

## Discussion

PGE$_2$ is a cyclooxygenase-derived product of arachidonic acid metabolism that plays a major role in regulating such diverse physiological processes as smooth muscle tone, inflammation, and pain (reviewed in ref. 17). The biological effects of PGE$_2$ are often multifaceted and can appear contradictory to traditional signaling paradigms. As introduced earlier, some of these properties of PGE$_2$ are due to the fact that it is an endogenous agonist for 4 receptor subtypes coupled to several signal transduction cascades. The EP$_1$ receptor is linked to IP$_3$ and [Ca$^{2+}$]$_i$ turnover through G$_q$-mediated signal transduction (18), whereas the EP$_2$ and EP$_4$ receptors stimulate adenylyl cyclase and cAMP produc-

tion through G$_s$ (19–21). Splice variants of the EP$_3$ receptor give rise to multiple isoforms that apparently can couple to G$_i$, G$_s$, or G$_q$ (22, 23). Since one or more of these receptors may be expressed by a cell or tissue, the integrated response to PGE$_2$ often represents the net effect of additive or opposing signal transduction events. Moreover, temporal and spatial changes in patterns of EP receptor expression in response to various stimuli (e.g., injury and inflammation) provide an additional level of dynamic regulation and complexity to PGE$_2$-regulated processes in the airways. For example, recent studies of the PGE$_2$-mediated fibroproliferative response due to intratracheal bleomycin have shown an approximately 50% decrease in fibroblast EP$_2$ receptor mRNA without significant change in the other EP subtypes (24), whereas FITC-mediated fibrosis was associated with decreases in both EP$_2$ and EP$_4$ transcript expression (24).

Because PGE$_2$ is produced endogenously within the lung and activates pathways that may both enhance and inhibit ASM contraction, it may have particular relevance in asthma. PGE$_2$ is produced by ASM cells, bronchial and alveolar epithelial cells, fibroblasts, and inflammatory cells in the lung, and increased levels have been reported in some studies with human asthma (25, 26). Furthermore, an initial enzyme for prostanoid receptor synthesis (COX-2), as well as PGE$_2$ precursors, are increased in asthmatic airways (27, 28). Following its discovery, PGE$_2$ was found to relax ASM and thus has generally been considered to be a bronchoprotective prostanoid. The bronchodilatory effect of PGE$_2$ appears to be due to activation of the EP$_2$ receptor subtype, since PGE$_2$-mediated bronchodilation is present in EP$_1$-, EP$_3$-, and EP$_4$-null mice but absent in EP$_2$-null mice (29). Interestingly, in nonasthmatic humans, PGE$_2$ exerts a net bronchodilation; in asthmatics, though, the response is highly variable, sometimes resulting in significant bronchoconstriction (30). The complex nature of PGE$_2$ action in the asthmatic milieu is further illustrated in that it may serve as an intermediary through which inflammatory cytokines can modulate other receptor systems that govern airway tone. In particular, PGE$_2$ appears to mediate the inhibitory effects of the inflammatory cytokines TGFβ and interleukin-1 on β$_2$AR signal transduction in cultured ASM (31–34). These inflammatory cytokines stimulate COX-2 and production of PGE$_2$ by ASM, and it has been proposed that the resulting increase in cAMP production following EP$_2$ receptor activation leads to desensitization of the β$_2$AR (3). However, the mechanism(s) by which this inhibition occurs has not been completely elucidated, nor has the role of other EP receptor subtypes in mediating this effect been explored.

We define here a unique role for the EP$_1$ receptor expressed on ASM cells using both molecular studies in transfected cells and ASM cells and physiologic studies in trachea. We showed that the EP$_1$ receptor existed as a heterodimer (or higher-order oligomer) with the β$_2$AR, and the signaling of this complex was manifested by an altered β$_2$AR conformation and decreased functional interaction with G$_{\alpha s}$. EP$_1$ activation by agonist further enhanced β$_2$AR desensitization, as shown in the [$^{35}$S]GTPγS studies. This effect was also readily observed in ASM cells utilizing whole-cell cAMP measurements and membrane [$^{35}$S]GTPγS binding and manifested at the physiologic level with intact tracheal rings. Interestingly, the extent of β$_2$AR desensitization evoked by the EP$_1$ agonist, as assessed using these distinctly different methods, amounted to approximately 50% in all cases. In addition, the EP$_1$ receptor, while capable of stimulating intracellular IP$_3$ and [Ca$^{2+}$]$_i$ (as assessed by global whole-cell assays), did not ultimately cause significant ASM

contraction. Thus the dimer may serve not only to form a specialized signaling unit, but could also place the complex in a subcellular compartment that isolates it from activation of the downstream components of contraction. Indeed, $\beta_2$ARs have been shown to be localized to caveolae, which are specialized flask-shaped invaginations of the cell membrane that promote association of the receptor with certain signal transduction elements (35). However, we note that $EP_1$ receptor–mediated contraction has been observed in guinea pig trachea (36), suggesting that the extent of $EP_1$-mediated tracheal contraction may depend on the species.

We have thus considered the physiologic role of the $EP_1$ receptor in ASM as *primarily* one of modulating $\beta_2$AR function, with no observable direct effect on contraction. To our knowledge, this "monitor-like" function has not been previously described for a 7-TM receptor with its heterodimeric partner. However, there are somewhat analogous scenarios with other receptors. For the GABAb R1 and R2 subtypes, it appears that the R1:R2 heterodimer represents a distinct signaling unit, in that the R1 subtype binds the agonist while the R2 subtype couples to G protein activation (37). Furthermore, GABAb R1 cell surface expression requires heterodimer formation with GABAb R2 in the endoplasmic reticulum (38). For the $\alpha_{1D}$AR, cell surface expression appears to be dependent on oligomeric association with the $\alpha_{1B}$AR (39). Once so expressed, each subtype can signal independently. Similarly, the $\beta_2$AR can form dimers with the $\alpha_{1D}$AR and promote its expression (40). Other examples of homo-and heterodimerization function have been recently reviewed (12, 15, 16). We are unaware of a previous report of the unique function of a 7-TM receptor that we describe here.

In the current report, we utilized the physiologic readout of airway contraction and relaxation as the relevant functional signal and found that activation of the $EP_1$ receptor had no direct physiologic action. However, we found that $EP_1$ activation resulted in substantial loss of $\beta_2$AR-mediated ASM relaxation. We demonstrated that this interaction of signal transduction networks occurred at the level of the receptors, rather than downstream effectors, and was not due to posttranslational modification of the $\beta_2$AR by phosphorylation or other potential distal-pathway crosstalk mechanisms (41). Rather, formation of the $EP_1$:$\beta_2$AR heterodimer was a distinct signaling complex, where the $EP_1$ receptor modulates $\beta_2$AR coupling to $G_{\alpha s}$. Using multiple approaches, the $EP_1$-agonist dependency of the $\beta_2$AR modulation was demonstrated. However, we cannot exclude the notion that the mere presence of the heterodimer acts to modulate the function of one of its members, the $\beta_2$AR. Indeed, the $[^{35}S]$GTP$\gamma$S binding studies showed that $\beta_2$AR coupling to $G_{\alpha s}$ was decreased when coexpressed with the $EP_1$ receptor. However, the spontaneous switching of the $EP_1$ receptor to the active conformation may mimic the agonist-occupied form; thus it is not unexpected that coexpression, particularly at relatively high levels, would have an agonist-occupied effect. Regardless, in the native state both receptors were expressed on ASM, and we showed that $EP_1$ receptor activation decreased $\beta_2$AR function in isolated ASM cells and in intact tissue.

In summary, we define a unique modulatory function of the $EP_1$ receptor, which acts primarily to regulate $\beta_2$AR function. In asthma, then, local concentrations of elevated $PGE_2$ could act to quench $\beta_2$AR function, resulting in decreased responsiveness to $\beta$-agonist. The mechanism of this receptor interaction appears to be due to the formation of a heterodimer; thus the $EP_1$:$\beta_2$AR dimer should be considered the functional signaling complex in ASM,

with a unique phenotype based on steric interactions that lead to attenuated $\beta_2$AR-$G_{\alpha s}$ coupling.

## Methods

*Plasmid constructs, cells culture, and transfection.* The human $\beta_2$AR cDNA was tagged at the amino terminus with the FLAG epitope and fused at the carboxyl terminus with the cDNA for Rluc, and the cDNA for the human $EP_1$ receptor was fused at the carboxyl terminus with the cDNA for YFP, using standard techniques. The final constructs representing $\beta_2$AR, FLAG-$\beta_2$AR, and $\beta_2$AR-Rluc were in pcDNA3, and the $EP_1$-YFP construct was in pEYFP-N1 (BD Biosciences — Clontech). Primary cultures of ASM cells were derived from explants of excised tracheas from the mice as reported previously (42) and maintained in DMEM, 10% FCS, and ×1 antibiotic-antimycotic solution (Invitrogen Corp.) at 37°C in a 95% air, 5% $CO_2$ incubator. These cells maintain the morphologic and immunohistochemical characteristics of ASM cells for at least 15 passages, although most experiments were performed with cells in passages 4–12. Both COS-7 and HEK 293 cells were similarly maintained as monolayers in DMEM supplemented with 10% FCS, 100 U/ml penicillin, and 100 mg/ml streptomycin. Transfection of these cells for BRET and $[^{35}S]$GTP$\gamma$S binding experiments was performed using Lipofectamine (Invitrogen Corp.) by methods previously described (43).

*RT-PCR.* Total RNA was extracted from freshly isolated lungs with Tri-Reagent (Molecular Research Center Inc.). An aliquot of RNA was reverse transcribed with random hexamers with murine leukemia virus reverse transcriptase (PerkinElmer) as previously described (43). Transgene cDNA was amplified with 150 nM each of a sense primer (5′-CGTGTCATTTCCT-GGGTGGCT-3′) and an antisense primer homologous to regions within the mouse $EP_1$ open reading frame (5′-GTGGCTGTGGCTGAAGTGATG-3′). PCR was at 95°C for 120 seconds followed by amplification for 35 cycles at 95°C for 60 seconds and 56°C for 60 seconds and a final extension at 72°C for 7 minutes. The PCR products were detected in agarose gels stained with ethidium bromide. RNA samples not subjected to reverse transcription were used as negative controls to ensure that the observed PCR product was not the result of contaminating DNA.

*Measurement of inositol phosphate production and $[Ca^{2+}]_i$.* Formation of $[^3H]$-inositol phosphate was determined in intact ASM cells as previously reported (41). Briefly, near-confluent ASM cells in 12-well plates were incubated with inositol-free media containing $[^3H]$-myoinositol (5 μCi/ml) for 24 hours at 37°C in 5% $CO_2$ atmosphere. Cells were then washed and incubated with PBS for 30 minutes followed by a 30-minute incubation with 20 mM LiCl in PBS. The cells were treated with either PBS (basal), 1 μM $PGE_2$, 1 μM 17-PTP, or thrombin (a positive control) for 15 minutes, after which total inositol phosphates were extracted by column chromatography with AG1-X8 resin (Bio-Rad).

To measure $[Ca^{2+}]_i$, murine ASM cells were seeded into black-walled, clear-based 96-well plates (Corning) at a density of approximately 80,000 cells per well and cultured overnight in 100 μl DMEM supplemented with 10% FCS as above. On the following day, the cells were incubated at 37°C for 60 minutes with the Calcium 3 indicator (Molecular Devices) that was dissolved in Hank's balanced salt solution containing 20 mM HEPES, pH 7.4, and 2.5 mM probenecid in a final volume of 200 μl/well. The cell plates were then placed into the FlexStation II scanning fluorimeter/luminometer (Molecular Devices) to monitor fluorescence before and after the addition of 50 μl vehicle or a ×5 concentration of the indicated drug (Figure 1, C and D) using an excitation wavelength of 485 nm, emission wavelength of 525 nm, and emission cutoff of 515 nm. Responses were measured as peak fluorescence intensity minus basal fluorescence intensity, with each data point in an individual experiment representing the mean of 4 replicates. Final data reported represent the mean of 4 different experiments using ASM cells derived from 2 different mice.

*Radioligand binding and cAMP production.* The expression of $\beta_2ARs$ in membranes prepared from transiently transfected HEK 293 and COS-7 cells was quantified by radioligand binding assays using the antagonist [$^{125}I$]-iodocyanopindolol as previously reported (44). To assess the rate of $\beta_2AR$ sequestration in ASM cells, whole-cell binding assays were performed using the hydrophilic, membrane-impermeant radioligand [$^3H$]-CGP-12177 to determine the amount of cell-surface $\beta_2AR$ in the untreated cells as well as in cells treated with either isoproterenol or isoproterenol with 17-PTP (1 μM each) for periods up to 30 minutes as previously described in detail (45).

To measure cAMP production, ASM cells were seeded onto 24-well plates and maintained overnight in DMEM supplemented with 10% FCS to allow adherence. The cells were then switched to serum-free DMEM for an additional 24 hours. The cells were loaded with [$^3H$]-adenine (2 μCi/well) for 2 hours and then washed twice with PBS to remove excess adenine. Cells were then treated with either vehicle or 17-PTP (1 μM final concentration) for 15 minutes before stimulation with either 1 μM isoproterenol or 100 μM forskolin for 15 minutes. Reactions were terminated by the addition of 50 μl concentrated HCl. After the samples were frozen and thawed once to ensure cell lysis, cAMP was eluted by alumina column chromatography. Recovered counts were corrected for adenine uptake, and column efficiency ascertained with tracer [$^{14}C$]-cAMP. Each data point was determined from the mean of triplicate samples, and expressed as its percentage of the mean forskolin response for that experiment. The results shown represent the mean ± SEM of 4 separate experiments performed with cell lines derived from 2 different mice.

*Tracheal ring contractility studies.* Studies of mouse tracheal ring contractility were performed as reported previously in detail (41). Briefly, tracheas were excised and dissected free of surrounding tissues and cut into rings of 5 mm in length. The rings were mounted on stainless steel wires connected to isometric force transducers and immersed in a physiologic saline solution (118 mM NaCl, 11 mM glucose, 4.73 mM KCl, 1.2 mM MgCl$_2$, 0.026 mM EDTA, 1.2 mM KH$_2$PO$_4$, 2.5 mM CaCl$_2$, and 25 mM NaH$_2$CO$_3$) at 37°C and bubbled with 95% O$_2$ and 5% CO$_2$, maintaining a pH of 7.40. Each tracheal ring was stretched to a tension of 5 mN, which we have previously determined to be an optimal passive tension for maximizing active force (42). Following a period of equilibration for 30 minutes, the indicated agents (Figures 2 and 3) were added to the bath, and the maximal response over the next 5 minutes was recorded. Cumulative concentration-isometric force curves were generated for the responses using standard curve-fitting techniques. Pretreatments of equilibrated rings included 1 μM 17-PTP for 15 minutes, 10 nM PGE$_2$ for 15 minutes, 10 μg/ml pertussis toxin for 4 hours, 100 μM L-NAME for 30 minutes, 10 μM indomethacin for 30 minutes, 5 μM U73112 for 15 minutes, and 10 μM Et-18-OCH$_3$ for 30 minutes. All mouse studies were reviewed and approved by the University of Cincinnati College of Medicine Animal Care and Use Committee.

*Receptor phosphorylation.* Whole-cell phosphorylation experiments were performed as previously described (46), with minor modifications. HEK 293 cells cotransfected with the $\beta_2AR$-FLAG and EP$_1$-YFP constructs were plated in 100-mm dishes. Forty-eight hours after transfection, the media was changed to serum- and phosphate-free DMEM containing 500 μCi/ml $^{32}P$-orthophosphate. After incubation for 2 hours at 37°C in 95% air and 5% CO$_2$, the cells were treated with vehicle, 1 μM isoproterenol, 100 nM phorbol-12-myristate-13-acetate, 1 μM 17-PTP, or 1 μM isoproterenol plus 1 μM 17-PTP for 15 minutes. The cells were then washed 4 times with ice-cold PBS and solubilized by rotating for 2 hours at 4°C in solubilization buffer, which consisted of 1% Triton X-100 (Sigma-Aldrich), 0.05% SDS, 0.5 mM EGTA, 1 mM EDTA, the phosphatase inhibitors sodium pyrophosphate and NaF (both at 10 mM), and the protease inhibitors leupeptin, aprotinin, benzamidine and soybean trypsin inhibitor (5 μg/ml each) in PBS. The lysates were centrifuged at 20,000 *g* for 10 minutes at 4°C

to remove unsolubilized material. $\beta_2AR$-FLAG was immunoprecipitated by incubating the solubilized lysate overnight at 4°C with an anti-FLAG antibody preconjugated to agarose beads (Sigma-Aldrich). After washing the beads 4 times with ice-cold solubilization buffer, the tagged receptor was eluted with 3× FLAG peptide (Sigma-Aldrich). The eluate was fractionated by 10% SDS-PAGE, and the resultant signal from the dried gel was quantified by a GE Healthcare phosphorimager. Data was expressed as relative units from the pixel densities using ImageQuant software (version 1.2).

*BRET measurements.* BRET assays were carried out with the Flexstation II scanning fluorimeter/luminometer (Molecular Devices) using methods similar to that previously reported by Bouvier et al. (14). HEK 293 cells either transfected with $\beta_2AR$-Rluc alone or cotransfected with receptor-YFP fusion constructs were detached 48 hours after transfection and seeded onto 96-well plates at a density of approximately 80,000 cells/well in PBS containing 0.1% glucose. To determine the full spectrum of emission, light-emission acquisition (420–560 nm) was started 5 minutes after coelenterazine h (5 μM final concentration) was added. Emission values recorded at 475 nm and 530 nm after addition of coelenterazine h were used to determine the BRET ratio for each well. In some experiments, the transfected cells were treated with either isoproterenol or 17-PTP for 15 minutes prior to addition of coelenterazine h. The net BRET signal for each condition, performed in triplicate, was calculated by dividing the 530-nm emission of receptor-YFP by the 475-nm emission of the receptor-Rluc after subtracting the background signal determined from cells transfected with the receptor-Rluc construct alone using the formula $[(Em_{530} - Em_{475}) \times CF]/EM_{475}$, where CF represents $Em_{530}/Em_{475}$, the ratio of the signals from cells expressing receptor-Rluc alone. Maximal BRET levels (BRET$_{max}$) were obtained by cotransfecting increasing levels of receptor-YFP constructs with a constant quantity of the $\beta_2AR$-Rluc construct. BRET$_{max}$ and BRET$_{50}$ were derived from fitting these data to a 1-site hyperbolic function.

*Immunoprecipitation and Western blotting.* HEK 293 cells expressing the EP$_1$ receptor, FLAG-tagged $\beta_2AR$, or both were solubilized for 2 hours at 4°C in RIPA buffer (1× PBS, 1% IGEPA, 0.5% sodium deoxycholate, and 0.1% SDS) containing protease inhibitors. The solubilized lysates were cleared by centrifugation at 10,000 *g*, and a portion of the cleared sample was removed for protein determination and Western blot analysis. The remainder was incubated with M2 anti-FLAG affinity matrix (Sigma-Aldrich) overnight at 4°C. The resin was then collected by centrifugation, washed 3 times with Tris-buffered saline, and eluted with 2× Laemelli loading buffer. For Western blot analysis, whole cell lysates and immunoprecipitated samples were fractionated on 8% polyacrylamide gels and transferred to PVDF membranes. Blots were blocked with 5% nonfat milk and incubated overnight at 4°C with a polyclonal anti-EP$_1$ antibody (Cayman Chemical Co.) diluted 1:200. The blots were then washed, incubated with anti-rabbit IgG antibody diluted 1:6,500 at room temperature for 1 hour, and detected by enhanced chemiluminesence.

*[$^{35}S$]GTPγS binding.* [$^{35}S$]GTPγS binding assays were performed as described previously (47) with modifications that include a G$_{\alpha s}$ immunoprecipitation step (48). HEK 293 cells were cotransfected with plasmid vectors encoding human G$_{s\alpha}$ and either $\beta_2AR$ alone or $\beta_2AR$ plus the EP$_1$ receptor. Studies with ASM cells were carried out without transfections utilizing endogenous expression of the receptors and G$_{s\alpha}$. For the binding reaction, partially purified cell membrane protein (~75 μg) was incubated for 15 minutes at 30°C in a binding buffer (10 mM HEPES, pH 7.4, 3 mM MgCl$_2$, and 50 mM NaCl) that included 50 nCi [$^{35}S$]GTPγS and 10 μM guanosine diphosphate in a total volume of 100 μl. Basal (vehicle) and agonist-stimulated (1 μM isoproterenol) conditions were each determined in the absence and presence of 1 μM 17-PTP. Parallel assays containing unlabeled GTPγS (100 μM) were used to define nonspecific binding.

The reactions were stopped by addition of cold solubilization buffer (10 mM HEPES, pH 7.4, 50 mM NaCl, 5 mM EDTA, and 0.5% Triton-X) and rotated for 2 hours at 4°C. After centrifugation at 20,000 $g$ for 15 minutes, the supernatant was incubated overnight with 1 μg $G_{\alpha s}$ antibody (Santa Cruz Biotechnology Inc.) and 20 μl protein A–conjugated agarose beads. The beads were washed 3 times with phosphorylation solubilization buffer, and the bound radioactivity was measured in a liquid scintillation counter. Under these conditions, nonspecific binding was typically <10% of the total. Agonist-stimulated binding was derived by subtracting the counts of basal samples from the counts of the isoproterenol-treated samples. Each data point within an experiment was determined from triplicate samples.

*Immunofluorescence microscopy*. Murine ASM cells were passed to Lab-Tek chamber slides (Nunc) and grown overnight. After the media was aspirated, the cells were washed with PBS and then fixed with cold methanol for 4 minutes. Cells were then placed in blocking buffer composed of PBS containing 10% donkey serum and 1% Triton-X for 30 minutes at room temperature. The blocking buffer was removed, and cells were incubated overnight at room temperature in PBS containing 1% Triton-X, a 1:50 dilution of a rabbit anti-EP$_1$ antibody (Santa Cruz Biotechnology Inc.), and a 1:200 dilution of a chicken anti-β$_2$AR antibody (Abcam). Primary antibody was not added to the negative controls. After incubation, the buffer containing the primary antibodies was aspirated, and the cells were washed with PBS containing 0.1% Triton-X. Cells were then incubated with secondary antibodies for 2–4 hours with 0.1% Triton-X in PBS containing a 1:200 dilution of a Cy2-conjugated donkey anti-rabbit antibody and a 1:800 dilution of a Cy3-conjugated donkey anti-chicken antibody. Cells were then washed with PBS and mounted with Gelmount (Biomeda) to reduce fading. Fluorescent images were captured electronically using the appropriate filter sets on a Zeiss Axioplan II Microscope System at a magnification of ×200.

*Statistics*. Concentration-response and BRET data were fit by nonlinear functions using the Prism software program (version 4.0; GraphPad Software). Statistical comparisons were by paired or unpaired Student's $t$ tests as appropriate, with $P < 0.05$ considered significant. Data are represented as mean ± SEM of the indicated number of experiments.

1. Green, S.A., and Liggett, S.B. 1996. G protein coupled receptor signalling in the lung. In *The genetics of asthma*. S. Liggett and D. Meyers, editors. Marcel Dekker Inc. New York, New York, USA. 67–90.
2. Sweatman, W.J., and Collier, H.O. 1968. Effects of prostaglandins on human bronchial muscle. *Nature*. **217**:69.
3. Pang, L., Holland, E., and Knox, A.J. 1998. Role of cyclo-oxygenase-2 induction in interleukin-1beta induced attenuation of cultured human airway smooth muscle cell cyclic AMP generation in response to isoprenaline. *Br. J. Pharmacol.* **125**:1320–1328.
4. Delamere, F., et al. 1994. Production of PGE2 by bovine cultured airway smooth muscle cells and its inhibition by cyclo-oxygenase inhibitors. *Br. J. Pharmacol.* **111**:983–988.
5. Churchill, L., et al. 1989. Cyclooxygenase metabolism of endogenous arachidonic acid by cultured human tracheal epithelial cells. *Am. Rev. Respir. Dis.* **140**:449–459.
6. Ozaki, T., Rennard, S.I., and Crystal, R.G. 1987. Cyclooxygenase metabolites are compartmentalized in the human lower respiratory tract. *J. Appl. Physiol.* **62**:219–222.
7. Sheller, J.R., Mitchell, D., Meyrick, B., Oates, J., and Breyer, R. 2000. EP(2) receptor mediates bronchodilation by PGE(2) in mice. *J. Appl. Physiol.* **88**:2214–2218.
8. Henry, P.J., Rigby, P.J., and Goldie, R.G. 1990. Distribution of beta 1- and beta 2-adrenoceptors in mouse trachea and lung: a quantitative autoradiographic study. *Br. J. Pharmacol.* **99**:136–144.
9. Daaka, Y., Luttrell, L.M., and Lefkowitz, R.J. 1997. Switching of the coupling of the β$_2$-adrenergic receptor to different G proteins by protein kinase A. *Nature*. **390**:88–91.
10. De Blasi, A., Lipartiti, M., Motulsky, H.J., Insel, P.A., and Fratelli, M. 1985. Agonist-induced redistribution of beta-adrenergic receptors on intact human mononuclear leukocytes: redistributed receptors are nonfunctional. *J. Clin. Endocrinol. Metab.* **61**:1081–1088.
11. Angers, S., Salahpour, A., and Bouvier, M. 2002. Dimerization: an emerging concept for G protein-coupled receptor ontogeny and function. *Annu. Rev. Pharmacol. Toxicol.* **42**:409–435.
12. Bulenger, S., Marullo, S., and Bouvier, M. 2005. Emerging role of homo- and heterodimerization in G-protein-coupled receptor biosynthesis and maturation. *Trends Pharmacol. Sci.* **26**:131–137.
13. Breit, A., Lagace, M., and Bouvier, M. 2004. Hetero-oligomerization between beta2- and beta3-adrenergic receptors generates a beta-adrenergic signaling unit with distinct functional properties. *J. Biol. Chem.* **279**:28756–28765.
14. Angers, S., et al. 2000. Detection of beta 2-adrenergic receptor dimerization in living cells using bioluminescence resonance energy transfer (BRET). *Proc. Natl. Acad. Sci. U. S. A.* **97**:3684–3689.
15. Salahpour, A., Angers, S., and Bouvier, M. 2000. Functional significance of oligomerization of G-protein-coupled receptors. *Trends Endocrinol. Metab.* **11**:163–168.
16. Bouvier, M. 2001. Oligomerization of G-protein-coupled transmitter receptors. *Nat. Rev. Neurosci.* **2**:274–286.
17. Narumiya, S., Sugimoto, Y., and Ushikubi, F. 1999. Prostanoid receptors: structures, properties, and functions. *Physiol. Rev.* **79**:1193–1226.
18. Funk, C.D., et al. 1993. Cloning and expression of a cDNA for the human prostaglandin E receptor EP1 subtype. *J. Biol. Chem.* **268**:26767–26772.
19. Katsuyama, M., et al. 1995. The mouse prostaglandin E receptor EP2 subtype: cloning, expression, and northern blot analysis. *FEBS Lett.* **372**:151–156.
20. Breyer, R.M., et al. 1996. Cloning and expression of the rabbit prostaglandin EP4 receptor. *Am. J. Physiol.* **270**:F485–F493.
21. Regan, J.W., et al. 1994. Cloning of a novel human prostaglandin receptor with characteristics of the pharmacologically defined EP2 subtype. *Mol. Pharmacol.* **46**:213–220.
22. Namba, T., et al. 1993. Alternative splicing of C-terminal tail of prostaglandin E receptor subtype EP3 determines G-protein specificity. *Nature*. **365**:166–170.
23. Negishi, M., et al. 1995. Signal transductions of three isoforms of mouse prostaglandin E receptor EP3 subtype. *Adv. Prostaglandin Thromboxane Leukot. Res.* **23**:255–257.
24. Moore, B.B., et al. 2005. Bleomycin-induced E prostanoid receptor changes alter fibroblast responses to prostaglandin E2. *J. Immunol.* **174**:5644–5649.
25. Krawiec, M.E., et al. 2001. Persistent wheezing in very young children is associated with lower respiratory inflammation. *Am. J. Respir. Crit. Care Med.* **163**:1338–1343.
26. Profita, M., et al. 2003. Increased prostaglandin E2 concentrations and cyclooxygenase-2 expression in asthmatic subjects with sputum eosinophilia. *J. Allergy Clin. Immunol.* **112**:709–716.
27. Redington, A.E., et al. 2001. Increased expression of inducible nitric oxide synthase and cyclo-oxygenase-2 in the airway epithelium of asthmatic subjects and regulation by corticosteroid treatment. *Thorax*. **56**:351–357.
28. Taha, R., et al. 2000. Prostaglandin H synthase 2 expression in airway cells from patients with asthma and chronic obstructive pulmonary disease. *Am. J. Respir. Crit. Care Med.* **161**:636–640.
29. Tilley, S.L., et al. 2003. Receptors and pathways mediating the effects of prostaglandin E2 on airway tone. *Am. J. Physiol. Lung Cell. Mol. Physiol.* **284**:L599–L606.
30. Mathe, A.A., and Hedqvist, P. 1975. Effect of prostaglandins F2 alpha and E2 on airway conductance in healthy subjects and asthmatic patients. *Am. Rev. Respir. Dis.* **111**:313–320.
31. Vigano, T., et al. 1997. Cyclooxygenase-2 and synthesis of PGE2 in human bronchial smooth-muscle cells. *Am. J. Respir. Crit. Care Med.* **155**:864–868.
32. Belvisi, M.G., et al. 1997. Induction of cyclo-oxygenase-2 by cytokines in human cultured airway smooth muscle cells: novel inflammatory role of this cell type. *Br. J. Pharmacol.* **120**:910–916.
33. Fong, C.Y., Pang, L., Holland, E., and Knox, A.J. 2000. TGF-beta1 stimulates IL-8 release, COX-2 expression, and PGE(2) release in human airway smooth muscle cells. *Am. J. Physiol. Lung Cell. Mol. Physiol.* **279**:L201–L207.
34. Pang, L., and Knox, A.J. 1997. Effect of interleukin-1 beta, tumour necrosis factor-alpha and interferon-gamma on the induction of cyclo-oxygenase-2 in cultured human airway smooth muscle cells. *Br. J. Pharmacol.* **121**:579–587.
35. Steinberg, S.F. 2004. beta(2)-Adrenergic receptor signaling complexes in cardiomyocyte caveolae/

lipid rafts. *J. Mol. Cell. Cardiol.* **37**:407–415.

36. Ndukwu, I.M., White, S.R., Leff, A.R., and Mitchell, R.W. 1997. EP1 receptor blockade attenuates both spontaneous tone and PGE2-elicited contraction in guinea pig trachealis. *Am. J. Physiol.* **273**:L626–L633.

37. Galvez, T., et al. 2001. Allosteric interactions between GB1 and GB2 subunits are required for optimal GABA(B) receptor function. *EMBO J.* **20**:2152–2159.

38. Kuner, R., et al. 1999. Role of heteromer formation in GABAB receptor function. *Science.* **283**:74–77.

39. Hague, C., Uberti, M.A., Chen, Z., Hall, R.A., and Minneman, K.P. 2004. Cell surface expression of alpha1D-adrenergic receptors is controlled by heterodimerization with alpha1B-adrenergic receptors. *J. Biol. Chem.* **279**:15541–15549.

40. Uberti, M.A., Hague, C., Oller, H., Minneman, K.P., and Hall, R.A. 2005. Heterodimerization with beta2-adrenergic receptors promotes surface expression and functional activity of alph-

a1D-adrenergic receptors. *J. Pharmacol. Exp. Ther.* **313**:16–23.

41. McGraw, D.W., Almoosa, K.F., Paul, R.J., Kobilka, B.K., and Liggett, S.B. 2003. Antithetic regulation by β-adrenergic receptors of Gq-receptor signaling via phospholipase-C underlies the airway β-agonist paradox. *J. Clin. Invest.* **112**:619–626. doi:10.1172/JCI200318193.

42. McGraw, D.W., et al. 1999. Transgenic overexpression of β2-adrenergic receptors in airway smooth muscle alters myocyte function and ablates bronchial hyperreactivity. *J. Biol. Chem.* **274**:32241–32247.

43. Small, K.M., et al. 2004. Polymorphisms of the cardiac presynaptic α2Cadrenergic receptors: diverse intragenic variability with haplotype-specific functional effects. *Proc. Natl. Acad. Sci. U. S. A.* **101**:13020–13025.

44. Mialet-Perez, J., Green, S.A., Miller, W.E., and Liggett, S.B. 2004. A primate-dominant third glycosylation site of the β2-adrenergic receptor routes

receptors to degradation during agonist regulation. *J. Biol. Chem.* **279**:38603–38607.

45. Green, S., and Liggett, S.B. 1994. A proline-rich region of the third intracellular loop imparts phenotypic β1- versus β2-adrenergic receptor coupling and sequestration. *J. Biol. Chem.* **269**:26215–26219.

46. Jewell-Motz, E.A., Small, K.M., and Liggett, S.B. 2000. $\alpha_{2A}/\alpha_{2C}$-adrenergic receptor third loop chimera show that agonist interaction with receptor-subtype backbone establishes G protein-coupled receptor kinase phosphorylation. *J. Biol. Chem.* **275**:28989–28993.

47. Small, K.M., Forbes, S.L., Brown, K.M., and Liggett, S.B. 2000. An Asn to Lys polymorphism in the third intracellular loop of the human $\alpha_{2A}$-adrenergic receptor imparts enhanced agonist-promoted $G_i$ coupling. *J. Biol. Chem.* **275**:38518–38523.

48. Milligan, G. 2003. Principles: extending the utility of [35S]GTP gamma S binding assays. *Trends Pharmacol. Sci.* **24**:87–90.